

MedRep: Medical Concept Representations for General Electronic Health Record Foundation Models

Junmo Kim¹, Namkyeong Lee², Jiwon Kim³, Kwangsoo Kim^{4,5,6}

¹Interdisciplinary Program in Bioengineering, Seoul National University

²Dept. of Industrial and Systems Engineering, KAIST

³Interdisciplinary Program of Medical Informatics, Seoul National University

⁴Dept. of Transdisciplinary Medicine, ICMIT, Seoul National University Hospital

⁵Center for Data Science, Healthcare AI Research Institute, Seoul National University Hospital

⁶Dept. of Medicine, College of Medicine, Seoul National University

Abstract

Electronic health record (EHR) foundation models have been an area ripe for exploration with their improved performance in various medical tasks. Despite the rapid advances, there exists a fundamental limitation: Processing unseen medical codes out of vocabulary. This problem limits the generalizability of EHR foundation models and the integration of models trained with different vocabularies. To alleviate this problem, we propose a set of novel medical concept representations (MedRep) for EHR foundation models based on the observational medical outcome partnership (OMOP) common data model (CDM). For concept representation learning, we enrich the information of each concept with a minimal definition through large language model (LLM) prompts and complement the text-based representations through the graph ontology of OMOP vocabulary. Our approach outperforms the vanilla EHR foundation model and the model with a previously introduced medical code tokenizer in diverse prediction tasks. We also demonstrate the generalizability of MedRep through external validation. Our code implementation is publicly available at <https://github.com/kicarussays/MedRep>

Introduction

Electronic health records (EHRs) store a lot of data generated from a hospital, such as diagnoses, measurements, prescriptions, and procedures. Most tertiary hospitals in many countries have adopted EHRs to manage hospital data (Parasrampur and Henry 2019; Liang et al. 2021). With the widespread use of EHRs, numerous studies have utilized EHR data and machine learning techniques for tasks like medical event prediction (Huang et al. 2023), drug recommendation (Zhang et al. 2023a), and patient monitoring (Kim et al. 2024). With the availability of large patient data and the tremendous success of language models, developing EHR foundation models based on medical code and language models has become an area ripe for exploration (Li et al. 2020; Rasmy et al. 2021; Yang et al. 2023; Renc et al. 2024). The medical history of each patient can be represented as a sequence of medical codes, which is called a patient trajectory (Bornet et al. 2025). Each code and trajectory corresponds to a word and a sentence in natural language. Along with similar problem settings, EHR founda-

tion models have been trained to comprehend medical context by paradigms of language models and utilized to predict several medical events, such as in-hospital mortality, long length of stay, readmission, and various diseases (Li et al. 2020; Guo et al. 2024).

Despite the rapid advances, EHR foundation models have a fundamental limitation: The discrepancy of medical code vocabularies from different institutions. For example, suppose two hospitals store diagnosis records using different vocabularies SNOMED-CT (Donnelly et al. 2006) and ICD-10 (Quan et al. 2005), respectively. In this case, a model trained from one hospital may not operate at the other hospital because the unseen medical codes might be treated as unknown codes. To mitigate the difference in data, a lot of medical institutions have introduced an observational medical outcome partnership (OMOP) common data model (CDM), developed and maintained by the Observational Health Data Sciences and Informatics (OHDSI) initiative (Stang et al. 2010). This model enables the transformation of different EHR databases into a standardized format. Instead of directly relying on various medical vocabularies, such as SNOMED-CT (Donnelly et al. 2006), ICD-10 (Quan et al. 2005), RxNorm (Liu et al. 2005), and LOINC (McDonald et al. 2003), the OMOP CDM standardizes all those medical codes under a single unified vocabulary: the OMOP vocabulary. More than 9 million medical codes from dozens of medical vocabularies can be systemically mapped to standardized OMOP concept IDs. As a result, EHR foundation models built on OMOP CDM can seamlessly operate across any institution adopting the OMOP standard.

However, merging OMOP CDM-based EHR data across institutions is still hardly available due to patient privacy regulations. Thus, EHR foundation models built on OMOP CDM must be trained separately at each institution, even though they share a common data structure and vocabulary. Additionally, hospitals using OMOP CDM may use different concept IDs for the same concept (Kim et al. 2025). For instance, to map the prescription of aspirin 100MG, there exist diverse relevant concept IDs, such as 1113143 (aspirin 100MG Oral Tablet), 42483115 (Aspirin 100 MG Oral Capsule), 40012940 (Aspirin 100MG Oral Solution), 35136978 (Aspirin 100MG Oral Tablet by Pfizer), and 36893848 (Aspirin 100MG/ML Oral Solution). While these concepts are

similar, EHR foundation models may treat them differently because they are associated with distinct concept IDs and tokenized indices. As a result, when a model is transferred to other institutions, it may fail to recognize semantically similar but previously unseen concepts, limiting its ability to operate across external datasets generally.

In this study, we propose MedRep, a set of OMOP medical concept representations that can be directly utilized across any EHR foundation model. MedRep can replace traditional learnable token embeddings, preventing EHR foundation models from treating the embeddings of the same tokens differently. For MedRep training, we first generate brief descriptions of the clinical background and context for each concept using large language model (LLM) prompts (Schick and Schütze 2020). Next, we learn the generated descriptions through a masked language model (MLM) (Devlin et al. 2019) to produce text-based representations. These representations are then enhanced through graph representation learning and the graph ontology of the OMOP vocabulary. Through MedRep, we enhance the compatibility of EHR foundation models, enhancing downstream task performance in both internal and external validation. There exists concurrent work, MedTok (Su et al. 2025); however, it has not been explored to externally validate the performance using separate datasets. We compare the internal and external validation performance of EHR foundation models with no pretrained representations, with MedTok, and with MedRep.

Results

Data and target outcomes We used two publicly available EHR datasets: MIMIC-IV (version 2.2) (Johnson et al. 2023) and EHRSHOT (Wornow et al. 2023). To assess the compatibility of MedRep, we first pretrained and finetuned EHR foundation models on MIMIC-IV, then evaluated their predictive performance using the MIMIC-IV hold-out test set (internal validation) and the full EHRSHOT dataset (external validation), without any further parameter updates. Since EHRSHOT is originally formatted in OMOP CDM while MIMIC-IV is not, we converted the original MIMIC-IV into OMOP format using the official GitHub repository of OHDSI (<https://github.com/OHDSI/MIMIC>). We used four OMOP CDM tables, including condition occurrence, drug exposure, measurement, and procedure occurrence. For pretraining, we used 85% of the MIMIC-IV patients (70% for training and 15% for validation). The remaining 15% of patients were used for finetuning, which was further split into training, validation, and test (internal validation) sets at a 6:2:2 ratio. Since EHR foundation models rely on longitudinal clinical records, we included only patients who had been hospitalized for more than two days (Kim et al. 2025). Baseline characteristics of the datasets are summarized in Table 1. Both datasets contained approximately 26,000 medical concepts, and MIMIC-IV had a higher proportion of male patients compared to EHRSHOT (62.87% versus 54.60%, respectively).

The target outcomes for finetuning included three categories: clinical outcomes (Guo et al. 2023), patient phenotypes (Harutyunyan et al. 2019), and in-hospital events.

Table 1: Baseline characteristics of datasets.

	MIMIC-IV	EHRSHOT
Patients, n	257,992	4,403
Records, n	1,114,054,364	2,942,281
Visits, n	2,468,013	116,060
Concept IDs, n	26,894	26,303
Age, mean (std)	52.54 (20.89)	52.33 (17.31)
Male sex, n	62.87%	54.6%
Clinical outcomes, % (case / total)		
In-hospital mortality	3.68% (239 / 6499)	6.57% (289 / 4402)
Long length of stay	30.90% (2008 / 6499)	27.01% (1189 / 4402)
Readmission	2.02% (131 / 6499)	9.45% (416 / 4402)
Phenotypes, % (case / total)		
Acute and unspecified renal failure	10.41% (1280 / 12301)	7.27% (191 / 2628)
Acute cerebrovascular disease	4.38% (539 / 12301)	5.29% (139 / 2628)
Acute myocardial infarction	2.16% (266 / 12301)	2.97% (78 / 2628)
Cardiac dysrhythmias	14.08% (1732 / 12301)	18.42% (484 / 2628)
Chronic kidney disease	7.30% (898 / 12301)	7.80% (205 / 2628)
Chronic obstructive pulmonary disease	5.44% (669 / 12301)	5.63% (148 / 2628)
Complications of surgical/medical care	53.56% (6589 / 12301)	58.71% (1543 / 2628)
Conduction disorders	3.72% (458 / 12301)	7.80% (205 / 2628)
Congestive heart failure; nonhypertensive	7.39% (909 / 12301)	7.08% (186 / 2628)
Coronary atherosclerosis and related	10.85% (1335 / 12301)	10.01% (263 / 2628)
Diabetes mellitus with complications	11.61% (1428 / 12301)	11.30% (297 / 2628)
Diabetes mellitus without complication	63.21% (7775 / 12301)	37.06% (974 / 2628)
Disorders of lipid metabolism	19.34% (2379 / 12301)	17.16% (451 / 2628)
Essential hypertension	22.30% (2743 / 12301)	20.47% (538 / 2628)
Fluid and electrolyte disorders	12.63% (1554 / 12301)	10.84% (285 / 2628)
Gastrointestinal hemorrhage	2.72% (335 / 12301)	2.93% (77 / 2628)
Hypertension with complications	11.32% (1393 / 12301)	12.18% (320 / 2628)
Other liver diseases	25.28% (3110 / 12301)	37.48% (985 / 2628)
Other lower respiratory disease	28.02% (3447 / 12301)	36.95% (971 / 2628)
Other upper respiratory disease	35.50% (4367 / 12301)	39.92% (1049 / 2628)
Pleurisy; pneumothorax; pulmonary collapse	3.87% (476 / 12301)	9.32% (245 / 2628)
Pneumonia	3.63% (446 / 12301)	3.23% (85 / 2628)
Respiratory failure; insufficiency; arrest	3.93% (484 / 12301)	3.54% (93 / 2628)
Septicemia (except in labor)	4.05% (498 / 12301)	3.69% (97 / 2628)
In-hospital events		
Urinary tract infection	11.88% (2127 / 17906)	12.88% (482 / 3741)
Fracture	5.81% (1028 / 17680)	7.63% (290 / 3802)
Sepsis	8.85% (1599 / 18070)	18.28% (726 / 3972)
Pneumonia	11.80% (2110 / 17879)	19.34% (749 / 3872)
Myocardial infarction	2.80% (511 / 18258)	10.06% (393 / 3907)

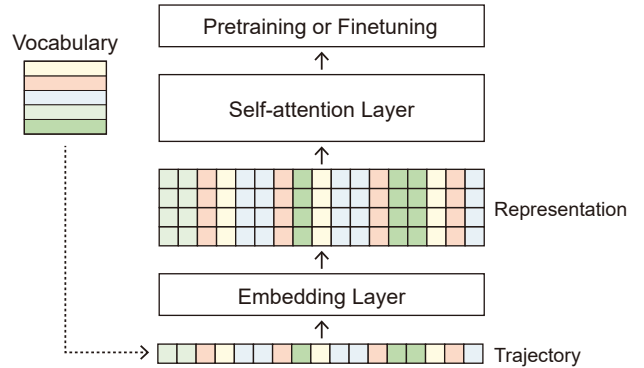


Figure 1: Basic structure of electronic health record foundation models. A patient trajectory is a sequence of medical code indices, which are transformed into embeddings by the embedding layer. The embedding layer, typically a matrix of vocabulary size by hidden dimension, functions as a lookup table that retrieves an embedding for each index. In conventional settings, the parameters of embedding layer are learnable and updated during training.

Clinical outcomes included in-hospital mortality (MT), long length of stay (LLOS), and readmission (RA). Patient phenotypes (Pheno) included 24 acute care conditions. In-hospital events consisted of urinary tract infection (UTI) (Møller, Sørensen, and Hardahl 2021), fracture (Fx) (Almog et al. 2020), sepsis (Nemati et al. 2018), pneumonia (PNA)

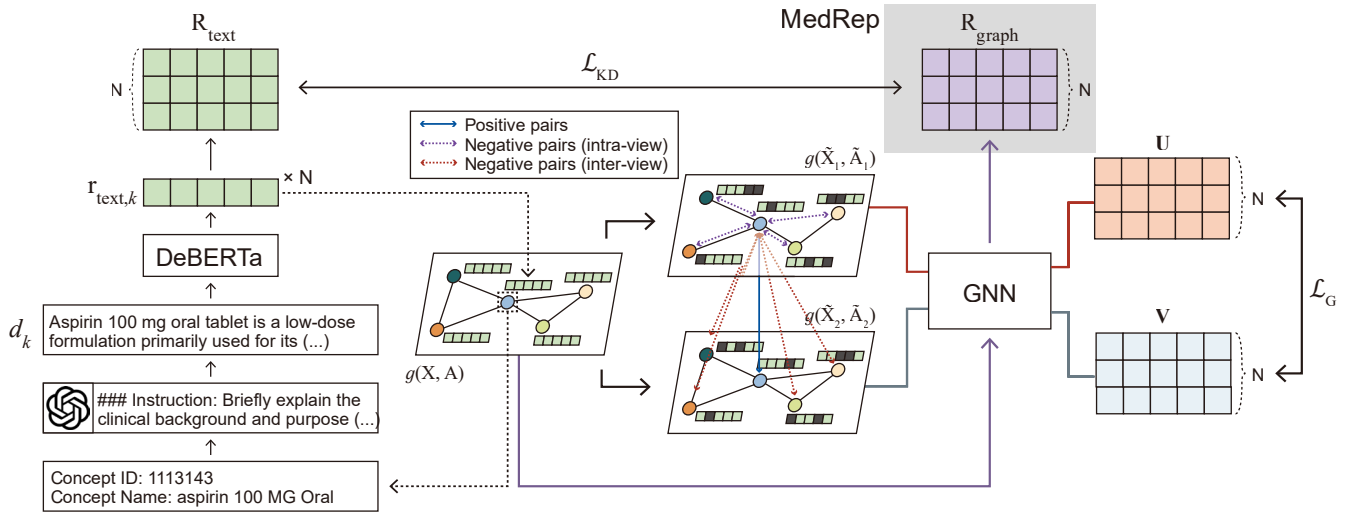


Figure 2: Medical concept representation learning process. For k -th medical concept with minimal textual definition, LLM-attributed description d_k is assigned. The description d_k is then encoded into a representation $r_{text,k}$ by a small language model (e.g., DeBERTa). Each $r_{text,k}$ serves a node feature of OMOP vocabulary relational graph. MedRep is trained by iteratively updating $r_{text,k}$ using both graph contrastive learning loss \mathcal{L}_G and knowledge distillation loss \mathcal{L}_{KD} . \mathcal{L}_{KD} is applied to prevent MedRep from forgetting information acquired from LLM-attributed descriptions.

(Effah et al. 2022), and myocardial infarction (MI) (Mandair et al. 2020). The incidence rates of these target outcomes are summarized in Table 1. Among the clinical outcomes, LLOS had the highest incidence rates in both hospitals, while MT and RA rates were higher in EHRSHOT than in MIMIC-IV. For phenotypes, the incidence rates of all phenotypes were higher than 2% for both datasets. Incidence rates of all in-hospital events were higher in EHRSHOT than MIMIC-IV. All target outcomes were labeled based on definitions from previous studies (Guo et al. 2023; Harutyunyan et al. 2019; Kim et al. 2025). Prediction timepoints were defined as follows: for MT and LLOS, predictions were made at midnight on the day of admission; for RA, at midnight on the day of discharge; for phenotypes, at midnight on the second day of admission; and for in-hospital events, one day prior to their occurrence.

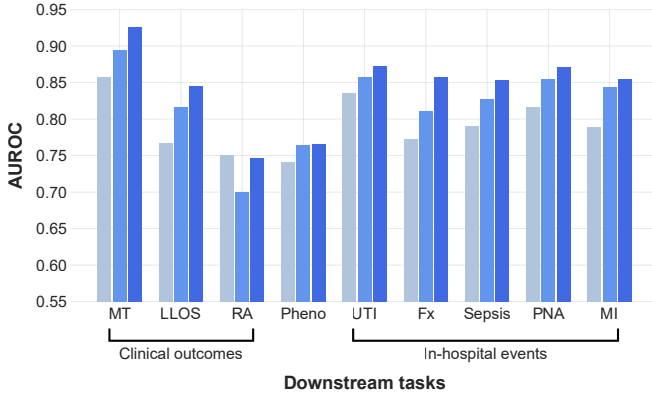
Medical concept representation (MedRep) MedRep is a set of medical concept representations. An EHR foundation model typically consists of embedding layers, self-attention layers, and subsequent components for pretraining or finetuning (Figure 1). The input to EHR foundation models is a sequence of medical code indices, which is called a patient trajectory, along with corresponding additional information such as age and time. Separate embedding layers exist for medical codes and for each additional information. Each embedding layer is a lookup table that maps an index to a numerical vector (embedding). For each point, all embeddings (e.g., medical code, age, and time) are summed and then pass through self-attention layers and subsequent pretraining or finetuning layers according to the objective. During pretraining or finetuning, all parameters of EHR foundation models, including the embedding layers, are updated. Each

embedding serves as a representation of the corresponding index. In contrast, our approach replaces the learnable embedding layer for medical codes with fixed, pretrained representations, MedRep.

Using phrase-level concept names and the graph ontology of OMOP vocabulary, we first created text-based representations by leveraging a language model along with LLM-attributed descriptions for each concept. These text-based representations were then enhanced by relational information between concepts, utilizing the graph ontology of OMOP vocabulary and graph contrastive learning (GCL) (Zhu et al. 2020). For GCL, we used the GRACE framework, where two different graph views are generated to optimize the pairwise objective, arranging positive pairs to be close and negative pairs to be apart (Zhu et al. 2020).

However, we observed that simply applying GCL led to representations that are extremely sparse and less informative. This phenomenon was because text-based representations were easily separable using only a few features, and our graph neural network (GNN) in GCL focused primarily on distinguishing positive and negative pairs rather than enriching current representations. This resulted in oversimplified embeddings that are easily separable but lack semantic detail. To address this problem, we adopted a knowledge distillation (KD) loss from Learning without Forgetting (LwF) (Li and Hoiem 2017), a continual learning method designed to prevent catastrophic forgetting (Goodfellow et al. 2015; McCloskey and Cohen 1989). MedRep was trained by iteratively minimizing the GCL loss and the KD loss, thereby capturing relational information from the OMOP graph ontology while preserving previously learned textual information. A brief illustration of our medical concept representation learning process is shown in Figure 2.

Internal validation



External validation

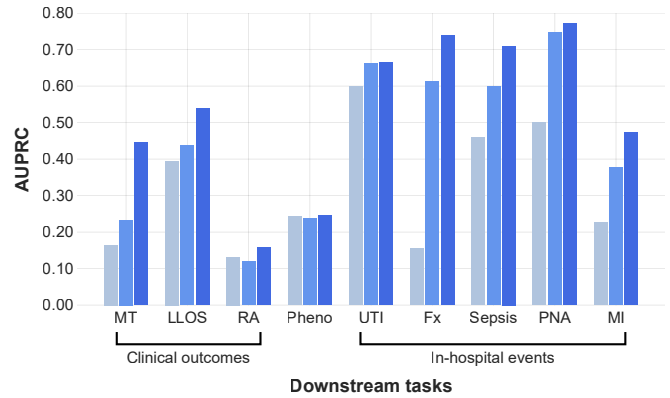
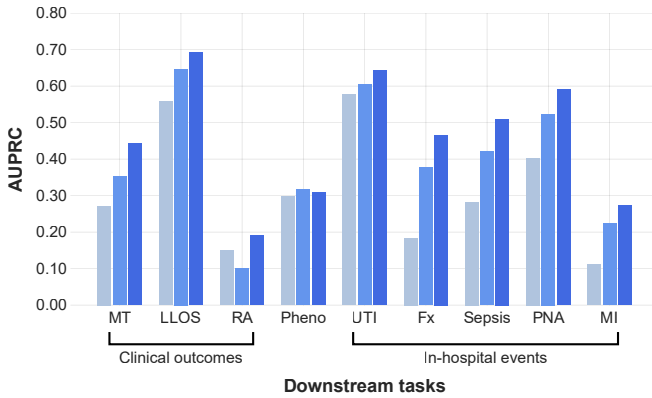
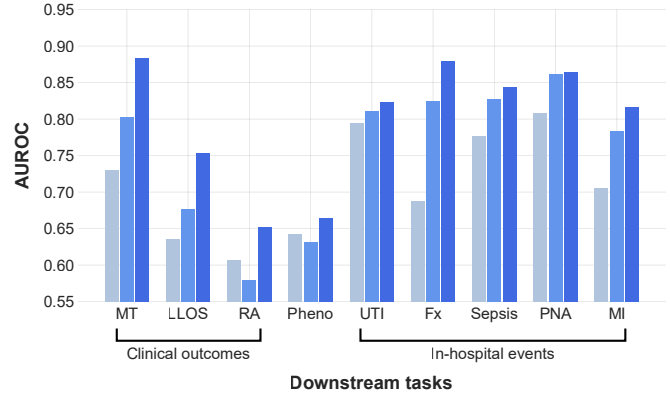


Figure 3: Downstream task performance. All downstream tasks were performed with three random seeds, and the reported AUROC and AUPRC values were averaged across these runs. Phenotype prediction is multilabel classification problem; therefore, we reported macro AUROC and macro AUPRC. All other tasks are binary classification problems.

Since MedRep is fixed and contains the clinical information of each concept, it not only improves the performance of EHR foundation models but also offers flexibility in coping with unseen concepts. We included 7,572,911 medical concepts, covering all medical codes from the condition, drug, measurement, and procedure domains of OMOP CDM. These concepts span 66 medical vocabularies, including SNOMED-CT (Donnelly et al. 2006), ICD-10 (Quan et al. 2005), ICD-9 (Quan et al. 2005), RxNorm (Liu et al. 2005), NDC (Food and of Drugs 1969), LOINC (McDonald et al. 2003), and HCPCS (Nusgart 2018).

Downstream task performance We evaluated the downstream task performance of EHR foundation models across three settings: without pretrained representations (vanilla), with MedTok, and with MedRep (Figure 3). BEHRT (Li et al. 2020) was used as the baseline architecture for the EHR foundation model. MedTok generally outperformed vanilla models in both internal and external validations, except for all RA and phenotype prediction tasks in external validation. MedRep achieved the best overall performance across

all downstream tasks, except for the area under the receiver operating characteristic curve (AUROC) for RA and the area under the precision-recall curve (AUPRC) for phenotype prediction in internal validation. Detailed performance metrics for all downstream tasks are summarized in Supplementary Table 1.

The performance improvements achieved by MedTok and MedRep are summarized in Table 2. Both methods enhanced the performance of EHR foundation models across most downstream tasks, with improvements mostly greater in external validation than in internal validation. This demonstrates that pretrained representations enhance not only the model performance but also its adaptability to new data. The improvements with MedRep were consistently greater than those with MedTok, indicating that MedRep can be a more effective option to enhance the generalizability of EHR foundation models.

Impact of graph ontology For MedRep, relational information among medical concepts was additionally learned by integrating the graph ontology of OMOP vocabulary

Table 2: Performance improvements achieved by MedTok and MedRep. Bold indicates the higher improvements.

		MT	LLOS	RA	Pheno	UTI	Fx	Sepsis	PNA	MI	Avg
<i>Metric: AUROC</i>											
Model	Validation										
MedTok	Internal	0.037	0.05	-0.051	0.023	0.021	0.039	0.037	0.038	0.055	0.028
	External	0.073	0.041	-0.027	-0.011	0.016	0.136	0.05	0.054	0.078	0.046
MedRep	Internal	0.069	0.078	-0.004	0.025	0.037	0.085	0.062	0.054	0.066	0.052
	External	0.153	0.117	0.045	0.021	0.028	0.191	0.067	0.057	0.111	0.088
<i>Metric: AUPRC</i>											
Model	Validation										
MedTok	Internal	0.081	0.089	-0.048	0.02	0.028	0.193	0.138	0.121	0.113	0.082
	External	0.068	0.043	-0.013	-0.006	0.062	0.457	0.139	0.246	0.15	0.127
MedRep	Internal	0.171	0.135	0.042	0.011	0.065	0.282	0.227	0.187	0.162	0.142
	External	0.28	0.144	0.026	0.003	0.065	0.583	0.251	0.271	0.245	0.208

Table 3: Performance variation with graph ontology. Bold indicates the best performance.

		MT	LLOS	RA	Pheno	UTI	Fx	Sepsis	PNA	MI	Avg
<i>Internal validation</i>											
Metric	Model										
AUROC	Vanilla	0.857	0.767	0.751	0.741	0.836	0.772	0.791	0.817	0.789	0.791
	No graph	0.926	0.845	0.737	0.771	0.86	0.848	0.861	0.869	0.871	0.843
	No LwF	0.916	0.823	0.727	0.765	0.86	0.85	0.846	0.856	0.84	0.831
	MedRep	0.926	0.845	0.747	0.766	0.873	0.857	0.853	0.871	0.855	0.844
AUPRC	Vanilla	0.272	0.558	0.149	0.297	0.577	0.184	0.283	0.403	0.111	0.315
	No graph	0.439	0.685	0.099	0.32	0.622	0.434	0.519	0.573	0.281	0.441
	No LwF	0.364	0.659	0.137	0.303	0.628	0.439	0.491	0.565	0.213	0.422
	MedRep	0.443	0.693	0.191	0.308	0.642	0.466	0.51	0.59	0.273	0.457
<i>External validation</i>											
Metric	Model										
AUROC	Vanilla	0.73	0.636	0.607	0.643	0.795	0.688	0.777	0.808	0.705	0.71
	No graph	0.864	0.735	0.621	0.66	0.801	0.86	0.858	0.869	0.826	0.788
	No LwF	0.778	0.7	0.596	0.635	0.797	0.864	0.8	0.855	0.75	0.753
	MedRep	0.883	0.753	0.652	0.664	0.823	0.879	0.844	0.865	0.816	0.798
AUPRC	Vanilla	0.165	0.395	0.132	0.243	0.599	0.155	0.459	0.501	0.227	0.32
	No graph	0.383	0.512	0.136	0.256	0.647	0.675	0.729	0.745	0.505	0.51
	No LwF	0.273	0.474	0.12	0.228	0.645	0.664	0.612	0.76	0.351	0.459
	MedRep	0.445	0.539	0.158	0.246	0.664	0.738	0.71	0.772	0.472	0.527

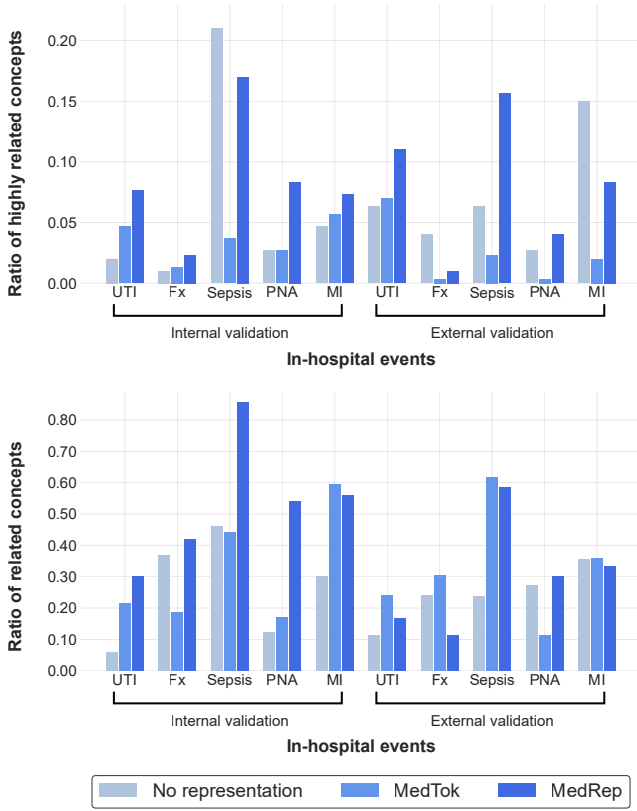


Figure 4: Ratio of highly related and related concepts. An LLM categorized the relevance of given concepts to the target outcome as *low*, *moderate*, and *high*. Highly related concepts include those labeled with *high*, and related concepts include those labeled with *high* or *moderate*. As we conducted experiments with three random seeds, we reported the average ratio.

with LLM-attributed text-based representations. As shown in Table 3, MedRep without the graph ontology (i.e., solely text-based representations) still outperformed vanilla models in both internal and external validation. Overall performance declined when MedRep was trained without LwF; however, MedRep trained with GCL combined with LwF improved average performance, especially in external validation. Specifically, MedRep exhibited consistent improvements in predicting clinical outcomes (MT, LLOS, RA), UTI, and Fx, while sepsis and MI were better with MedRep without the graph ontology.

Qualitative analysis We conducted a qualitative analysis using finetuned models for in-hospital events, as these outcomes generally have identifiable causes under common clinical backgrounds, whereas MT, LLOS, RA, and phenotypes are influenced by a wide variety of factors. Specifically, we extracted the top 100 most important concepts based on the attention scores of finetuned models, and used MedGemma-27B (Sellergrén et al. 2025) to classify their relevance to the target outcomes as low, moderate, or high. As shown in Figure 4, models with MedRep leveraged a

greater number of highly related concepts (labeled as high) for prediction compared to the other baselines, in six out of nine outcomes. Both MedTok- and MedRep-based models used a greater number of the related concepts (labeled as high or moderate) than the vanilla models.

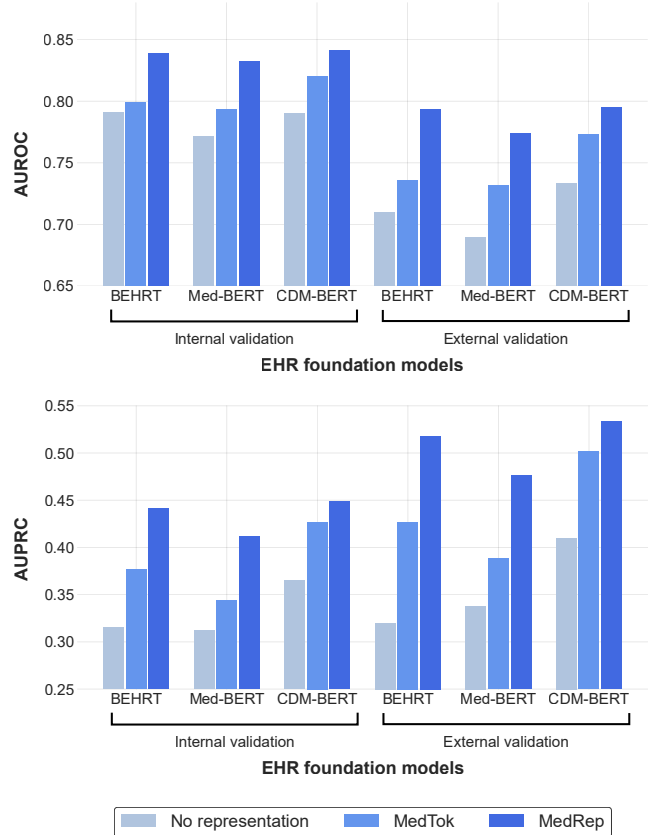


Figure 5: Downstream task performance on other EHR foundation models. All downstream tasks were performed with three random seeds, and the reported AUROC and AUPRC values were averaged across all experiments.

Scalability of MedRep To demonstrate the effectiveness of MedRep across diverse EHR foundation models, we further conducted experiments with Med-BERT (Rasmy et al. 2021) and CDM-BERT (Kim et al. 2025). Med-BERT additionally adopts a prolonged length of stay prediction process during pretraining to enhance the generalizability of the pre-trained model. CDM-BERT introduces domain embedding to indicate the domain of masked tokens during pretraining, to prevent the model from finding unnecessary medical concepts from other domains. For both Med-BERT and CDM-BERT, MedRep achieved the best overall performance, followed by MedTok (Figure 5). MedRep is applicable to any EHR foundation model that utilizes medical codes. Detailed performance values are summarized in Supplementary Tables 2 and 3.

Discussion

In this study, we introduced MedRep, a set of OMOP medical concept representations that can be directly integrated into any EHR foundation model to improve performance and generalizability. By leveraging an LLM and the graph ontology of OMOP vocabulary, we generated comprehensive medical concept representations. To address the oversimplification issue caused by GCL, we adopted a continual learning approach by incorporating the KD loss from LwF to retain knowledge learned from the LLM-attributed descriptions. MedRep consistently improved performance across diverse clinical tasks, especially in external validation. Furthermore, MedRep effectively identified features clinically related to target outcomes, enhancing the explainability of EHR foundation models. Finally, we demonstrated consistent performance of MedRep across diverse EHR foundation models.

Nowadays, most medical institutions are adopting EHR systems, and enormous amounts of healthcare data are accumulated every day (Liang et al. 2021). Despite this abundance, EHR data is generally not accessible to external researchers, and exporting EHR data is hardly available due to patient privacy regulations (d’Aliberti 2022). As a result, even though there have been a lot of studies that utilized EHR foundation models, they have typically utilized data from no more than three institutions (Guo et al. 2024). National claim data covering broader populations have been used in some cases; however, they lack detailed clinical observations such as continuous measurements (Gliklich, Leavy, and Dreyer 2019). To summarize, hospital EHR data is dense and high quality but small in scale and hardly sharable, whereas national claim data is large in scale but relatively low in quality. To enhance the generalizability and quality of EHR-based machine learning models, it is essential to merge the knowledge from multiple hospital datasets. In this context, MedRep offers an optimal solution, as it encourages similar concepts to have similar representations even if they have not been observed simultaneously. In addition, OMOP CDM has been applied to a lot of medical institutions (Reinecke et al. 2021; Biedermann et al. 2021), and machine learning models trained by OMOP CDM-based EHR data can be shared across institutions, because exporting only the weights of the model parameters is typically not restricted. Through MedRep, EHR foundation models developed at different institutions can cooperate to achieve general performance for various medical tasks. Therefore, MedRep can serve as a standard baseline representation for a large EHR foundation model.

As a prior work, MedTok (Su et al. 2025) has been proposed to quantize original medical codes into a unified codebook. MedTok is based on textual information for more than 600,000 medical codes from eight vocabularies and on relational knowledge from PrimeKG (Chandak, Huang, and Zitnik 2023). MedTok first generates text semantic and graph-level embeddings for modality-specific and cross-modality embeddings. Then, MedTok learns the codebook using those two embedding types and provides unified medical tokens for EHR foundation models. On the contrary, MedRep learns representations of medical concepts using

LLM-attributed textual information and OMOP graph ontology. MedRep consists of more than 7.5 million medical concepts from 66 medical vocabularies, which can be mapped from/to OMOP concepts, including measurement concepts such as laboratory tests and vital signs, which are not included in MedTok. The influence of graph ontology in MedRep was weaker than in MedTok; while MedTok aligns the representations from text and graph to be similar, we first trained text-based representations and then refined them using GCL and KD losses. This was because the relational information from OMOP vocabulary is limited to mapping and hierarchical information rather than the clinical relationship between concepts, whereas PrimeKG contains richer clinical relational information but does not cover all OMOP concepts. Our experiments exhibit that MedRep outperforms MedTok, demonstrating the effectiveness of MedRep in the OMOP CDM environment.

Although the influence of relational information was weaker than in the previous work (Su et al. 2025), the overall performance was greater with graph ontology, especially for predicting clinical outcomes. This suggests that medical concept representations enhanced with relational information can better capture factors contributing to complex outcomes. Meanwhile, the predictive performance of MedRep without the graph ontology was still comparable, allowing users to choose between the full MedRep and the graph-free version depending on their needs. Additionally, we experimented with combining the representations from MedRep and MedRep without a graph by summation, but this did not improve the performance.

One of the current challenges in EHR foundation models is explainability. Since EHR foundation models are based on self-attention architectures, most studies have provided qualitative analysis using attention scores from trained models, often supplemented by insights from clinicians or prior clinical research (Huang et al. 2023; Li et al. 2020; Kim et al. 2025). However, seeking advice from clinicians is costly and hardly available in real time, because clinicians should review the enormous records of patients. To address this problem, we used MedGemma-27B, a state-of-the-art LLM designed to interpret and reason about medical images and text (Sellersgren et al. 2025). For instance, MedGemma-27B identified the following concept IDs as highly related to UTI: 3004501 (Glucose [Mass/volume] in Serum or Plasma), 3037244 (Yeast [#/area] in Urine sediment by Microscopy high power field), 3004410 (Hemoglobin A1c/Hemoglobin.total in Blood), 4328657 (Color of Urine), 3022621 (pH of Urine by Test strip), 197320 (Acute kidney injury), 4193704 (Type 2 diabetes mellitus without complication), and 3021601 (Nitrite [Presence] in Urine by Test strip). All these concepts are well-established in the literature as closely associated with UTI (Scherstén and Fritz 1967; Guze and Haley 1958; Patterson and Andriole 1997; Levey and James 2017). While LLMs are excellent tools for providing general and comprehensible clinical information for users, they often struggle to reflect abundant clinical information from patient-specific longitudinal EHR data. On the other hand, EHR foundation models are adept at capturing individual complex medical histories for diverse specific

clinical tasks, but still face challenges in explainability. Considering MedGemma effectively identifies relevant concepts from EHR foundation models, MedRep-based EHR foundation models with LLM may create strong synergy, complementing each other.

This study has several limitations. First, we utilized only publicly available datasets, MIMIC-IV and EHRSHOT. It was to encourage reproducibility, but for further demonstration, it is essential to implement our approach to larger real-world datasets encompassing more diverse patient populations. Second, we did not use the observation table from OMOP CDM. The observation table contains clinical facts obtained in the context of examination, questioning, or a procedure, and any data that cannot be represented by existing domains, such as social and lifestyle facts, medical history, and family history. The data of the observation table usually consists of unstructured plain texts, and there is no standard for mapping those various records into standardized concepts. Representing and integrating these records into EHR foundation models remains future work. Third, we employed only the GRACE framework for GCL while there exist various other GCL methods. While the improvement by the graph ontology was observed, the gains were not significant across all tasks, indicating the need to investigate alternative approaches to better reflect relational information. Fourth, the downstream tasks were traditional, and the cohort definitions were not strictly defined by clinical experts. Further validation is required to determine if MedRep can be effective in more complex clinical tasks with strictly defined cohorts.

We suggest future work as follows: First, since MedRep covers dozens of medical vocabularies, developing dictionaries or tools that retrieve the appropriate representation for each code would be valuable. Second, exploring strategies to merge EHR foundation models from multiple institutions is important, as MedRep can standardize code systems across models, and many institutions are adopting OMOP CDM. Scaling laws (Kaplan et al. 2020) for EHR foundation models can be explored through the unified code system. Third, integrating PrimeKG with OMOP CDM could help enrich currently limited relational information of MedRep, as PrimeKG contains more clinically detailed relationships. Fourth, clinical context and hierarchical information contained in MedRep could be utilized beyond EHR foundation models, such as enhancing claim code systems used in hospitals and insurance, supporting healthcare policy development. Fifth, report-generating models for unstructured medical data (Liu et al. 2019; Wan et al. 2024) can be integrated into MedRep. Instead of simply concatenating the representations from multiple modalities, utilizing generated reports to create representations aligned with MedRep can contribute to building a multimodal EHR foundation model.

Methods

Concept curation For OMOP concepts, we extracted concept IDs from the central OHDSI vocabularies repository, Athena (<https://athena.ohdsi.org/search-terms/start>), which is regularly updated by the OHDSI community (Reinecke et al. 2021). We selected 7,572,911 concepts, each with a

concept name, from the drug, condition, measurement, and procedure domains, covering 66 medical vocabularies (summarized in Supplementary Table 4). Concepts from the condition, drug, and procedure were tokenized into their corresponding indices. For measurement concepts without numerical value, they were tokenized in the same way as for condition, drug, and procedure concepts. Each measurement concept with numerical values was divided into deciles, and the corresponding decile number (0-9) was appended to both the concept ID and the concept name. Finally, the dataset was expanded to 7,730,741 concepts after adding measurement concepts with deciles.

For the OMOP graph ontology, we excluded concepts with more than 100 links, as such concepts tend to be overly broad. These codes can be easily included via neighbor sampling, which may unintentionally allow marginal message passing during GCL. Examples of excluded nodes include dose form codes such as 46234469 (Injection) and 19082168 (Oral Capsule), as well as procedure group codes such as 42793831 (Surgery acts) and 42793832 (Act of anesthesia).

The final graph consisted of 5,129,561 nodes and 9,675,551 edges. Each edge has properties such as “is a”, “subsumes”, and “mapped from”, but for simplicity in implementing GCL, we regarded all edges as unattributed.

Prompt design for generating descriptions We enriched the clinical information of the given concepts using an LLM (Schick and Schütze 2020), because each OMOP concept has only minimal definitions, which are insufficient for generating representation with language models. In addition, the OMOP graph ontology generally includes hierarchical and mapping information between concepts, rather than cross-domain clinical relationships, such as which drugs are associated with specific conditions. Thus, the objective of generating LLM-attributed descriptions was to supplement each concept with richer textual clinical information, focusing on its cause, purpose, or context. For all domains, we instructed the LLM to describe the clinical background of each concept. Specifically, we requested information on treatments for conditions; the purpose and clinical meaning of ingredient, dosage form, and strength for drugs; the interpretation of each decile for measurements; and the clinical purpose of procedures. For drug concepts containing multiple substances, such as 45774969 (netupitant 300 MG / palonosetron 0.5 MG Oral Capsul), we requested comprehensive explanations covering all included drugs. We used ChatGPT-4o-mini (OpenAI Inc) for the LLM. The prompt for each domain and sample descriptions are provided in Supplementary Table 5.

MedRep: Medical concept representation learning For text-based representations, we trained a small language model based on masked language model (MLM) (Devlin et al. 2019) objective using the generated descriptions to encapsulate enriched clinical information. For each concept, the final text-based representation is denoted as $\mathbf{R}_{\text{text}} \in \mathbb{R}^{N \times h}$ where N is the vocabulary size and h is hidden dimension of the representation. We used DeBERTa (He et al. 2020) for small language model and enlarged the context length from 512 to 2048 tokens. The model was trained with

a batch size of 32 and a learning rate of 0.00005. We split \mathbf{R}_{text} into training and validation sets at an 8:2 ratio and validated the MLM loss every 200 training batches using 100 validation batches. Pretraining was terminated by early stopping with the patience of 30.

Even though similar concepts are expected to have similar description and similar text-based representations, we further refined these representations using the officially verified graph ontology of the OMOP vocabulary. Let the relational graph be $G = (C, E)$, where $C = \{c_k\}_{k=1}^N$ denotes the set of concepts (nodes) and $E \subseteq C \times C$ indicates the set of edges. The feature matrix and adjacency matrix are denoted as $X \in \mathbb{R}^{N \times h}$ and $A \in \{0, 1\}^{N \times N}$, where $X_k = r_{\text{text},k}$ is the text-based representation of the k -th concept, and $A_{ij} = 1$ if and only if $(c_i, c_j) \in E$. Our objective at this step was to train a GNN encoder g to produce final concept representations $R_{\text{graph}} = g(\mathbf{X}, \mathbf{A}) \in \mathbb{R}^{N \times h}$, as illustrated in Figure 2.

For GCL, we adopted the GRACE framework (Zhu et al. 2020), which is a general contrastive learning framework for unsupervised graph representation learning. GRACE generates two different graph views to obtain two embedding sets $U = g(\tilde{\mathbf{X}}_1, \tilde{\mathbf{A}}_1)$ and $V = g(\tilde{\mathbf{X}}_2, \tilde{\mathbf{A}}_2)$, where $\tilde{\mathbf{X}}$ and $\tilde{\mathbf{A}}$ are masked node features and dropped edges. We define the critic as $\theta(u, v) = s(p(u), p(v)) / \tau$, where s is the cosine similarity, p is a non-linear projection, and τ is a temperature parameter. The pairwise objective arranging positive pairs to be close and negative pairs to be apart for each positive pair $\mathbf{u}_k \in U$ and $\mathbf{v}_k \in V$ is

$$\ell(\mathbf{u}_k, \mathbf{v}_k) = \log \frac{e^{\theta(\mathbf{u}_k, \mathbf{v}_k)}}{\underbrace{e^{\theta(\mathbf{u}_k, \mathbf{v}_k)}}_{\text{positive pair}} + \underbrace{\sum_{i \neq k} (e^{\theta(\mathbf{u}_k, \mathbf{v}_i)} + e^{\theta(\mathbf{u}_k, \mathbf{u}_i)})}_{\text{inter- and intra-view negative pairs}}},$$

and the parameters of GNN encoder g are updated with the following objective to be minimized:

$$\mathcal{L}_G = -\frac{1}{2N} \sum_{k=1}^N [\ell(\mathbf{u}_k, \mathbf{v}_k) + \ell(\mathbf{v}_k, \mathbf{u}_k)].$$

The configuration for GRACE in this study is summarized in Supplementary Table 6. As representation learning involved more than 7.7 million concepts, allocating the whole feature matrix and adjacency matrix in memory was not possible. Instead, for each batch, we constructed a subgraph by extracting 30, 20, and 10 neighbors for 1-hop, 2-hop, and 3-hop connections from each node in the batch.

While GCL enhances the text-based representations via the OMOP graph ontology, the text-based representations are already highly informative, and the GNN might easily distinguish concepts resulting in loss of information (Zhang et al. 2023b). To mitigate this problem, we additionally trained the GNN with the scheme of LwF, a continual learning approach for maintaining previously learned information when training with new data. As a knowledge distillation loss \mathcal{L}_{KD} , we adopted Kullback–Leibler (KL) divergence loss between the original text-based representations

\mathbf{R}_{text} and the GNN-attributed representations $\mathbf{R}_{\text{graph}}$ as follows:

$$\mathcal{L}_{\text{KD}}(\mathbf{R}_{\text{text}} \parallel \mathbf{R}_{\text{graph}}) = \sum_{k=1}^N S(r_{\text{text},k}) \cdot \log \left(\frac{S(r_{\text{text},k})}{S(r_{\text{graph},k})} \right),$$

where $\mathbf{R}_{\text{text}} = \{r_{\text{text},k}\}_{k=1}^N$, $\mathbf{R}_{\text{graph}} = \{r_{\text{graph},k}\}_{k=1}^N = g(\mathbf{R}_{\text{text}}, \mathbf{A})$ and S is the softmax function. The parameters of GNN encoder g were alternately updated by minimizing \mathcal{L}_G and \mathcal{L}_{KD} . As a result, we obtained the final concept representation set $\mathbf{R}_{\text{graph}}$. EHR foundation models can directly use pretrained representations instead of training the embedding layer for medical concept indices.

Trajectory construction Each patient trajectory contains integer sequences of medical concept indices, age indices, visit indices, record indices, and domain indices, which are sorted in order of time. Each medical concept and age index refer to the corresponding concept and age. Each visit is assigned a unique visit index starting from 1 for each patient, and within each visit, the record index increments by 1 for each day, also starting from 1. The record index serves to encode temporal information for long visits. For CDM-BERT, domain index (ranging from 0 to 4) is assigned to every concept according to its domain (special token, condition, drug, measurement, and procedure). The embeddings of the concept itself, age, visit, record, and domain (for CDM-BERT) are summed and fed into the following layers. The maximum trajectory length was set to 2048. Every trajectory starts with the [CLS] token, and the [SEP] token was not used. Trajectories were padded by the [PAD] token with the maximum length.

Pretraining and finetuning details We used three EHR foundation models, BEHRT (Li et al. 2020), Med-BERT (Rasmy et al. 2021), and CDM-BERT (Kim et al. 2025). For pretraining, the trajectories with more than 2048 concepts are sliced into non-overlapping sub-trajectories with the maximum length to prevent potential dependency among trajectories from a single patient. The batch size and learning rate were set to 32 and 0.00005, respectively. We selected the pretraining models with the lowest MLM loss for 50 epochs with masked ratio of 0.3. AdamW optimizer (Loshchilov and Hutter 2017) was adopted for parameter update with a weight decay of 0.01. Pretraining was executed with 8 NVIDIA RTX A6000 GPUs for 2-3 days for each model.

For finetuning, the records before the prediction timepoint were utilized for prediction tasks, with the maximum length of trajectory 2048. For pretrained baseline models, a fully connected layer-based classification head was combined to predict the outcomes. We validated the model performance for every epoch and if the performance did not increase for 5 times, the finetuning process was terminated with early stopping. Each finetuning task was executed with a single NVIDIA RTX A6000 GPU for 4-8 hours. All finetuning tasks were performed with three random seeds, randomly splitting the training, validation, test sets of MIMIC-IV.

Outcome labeling For MT and LLOS, we used the last visit for each patient, excluding those who died on the day

of admission. LLOS was labeled for patients hospitalized more than one week. For RA, we randomly selected a visit except for the last visit and labeled patients who were hospitalized within one month after discharge. For phenotypes, since previous studies labeled them based on ICD-9 codes, we converted the code set for each phenotype into OMOP concepts, including all child codes. The prediction timepoint was set to midnight on the second day of admission. We selected the last visit with at least two days of hospitalization and excluded all patients who had at least one phenotype before the prediction timepoint. For each in-hospital event, including UTI, Fx, Sepsis, PNA, and MI, we first sorted the patients who had never suffered from the target outcome to form the control group and randomly selected a prediction timepoint for them. For the case group, we also randomly selected the day before the target outcome. For RA and in-hospital events, prediction timepoints were randomly assigned to minimize bias caused by our criteria.

MedTok training MedTok requires medical code description and local subgraph for each medical code. However, since our study used a different EHR format and medical code set, we generated MedTok using our pretrained text-based representations and the relational graph from the OMOP vocabulary, instead of using description text and PrimeKG. In our setting, covering OMOP concepts using PrimeKG, which contains around 130,000 nodes, was not feasible.

Qualitative analysis For qualitative analysis, we extracted the top 100 most important concepts from each in-hospital event prediction model. Specifically, for each patient, we obtained attention scores from the [CLS] token of the last self-attention layer. We then identified the top 100 concepts with the highest attention scores and counted how frequently each concept appeared in these top 100 lists across patients. Finally, we selected the 100 most frequently occurring important concepts for each model. Since all downstream tasks were run with three different random seeds, we combined the results and obtained the top 300 concepts for each in-hospital event. To evaluate the clinical relevance of these concepts, we instructed an LLM to classify each concept's relevance to the target outcomes as low, moderate, or high. The prompt used was: "We trained a machine learning model to predict [outcome] based on patients' past medical records. From this model, we extracted 100 important features. Now, we want to assess how strongly each of these features is related to [outcome]. Please evaluate each feature and categorize its relevance to [outcome] as one of the following: "Low", "Moderate", or "High". Make sure to provide an assessment for all 100 features — do not omit any. Please provide your answer in CSV format with two columns: feature, assessment. The extracted features are as follows: [100 extracted concepts]". For this task, we used MedGemma-27B (Søllergren et al. 2025), a state-of-the-art clinically specialized LLM.

References

- Almog, Y. A.; Rai, A.; Zhang, P.; Moulaison, A.; Powell, R.; Mishra, A.; Weinberg, K.; Hamilton, C.; Oates, M.; McCloskey, E.; et al. 2020. Deep learning with electronic health records for short-term fracture risk identification: crystal bone algorithm development and validation. *Journal of medical Internet research*, 22(10): e22550.
- Biedermann, P.; Ong, R.; Davydov, A.; Orlova, A.; Solovyev, P.; Sun, H.; Wetherill, G.; Brand, M.; and Didden, E.-M. 2021. Standardizing registry data to the OMOP Common Data Model: experience from three pulmonary hypertension databases. *BMC medical research methodology*, 21(1): 238.
- Bornet, A.; Proios, D.; Yazdani, A.; Santero, F. J.; Haller, G.; Choi, E.; and Teodoro, D. 2025. Comparing neural language models for medical concept representation and patient trajectory prediction. *Artificial Intelligence in Medicine*, 103108.
- Chandak, P.; Huang, K.; and Zitnik, M. 2023. Building a knowledge graph to enable precision medicine. *Scientific Data*, 10(1): 67.
- Devlin, J.; Chang, M.-W.; Lee, K.; and Toutanova, K. 2019. Bert: Pre-training of deep bidirectional transformers for language understanding. In *Proceedings of the 2019 conference of the North American chapter of the association for computational linguistics: human language technologies, volume 1 (long and short papers)*, 4171–4186.
- Donnelly, K.; et al. 2006. SNOMED-CT: The advanced terminology and coding system for eHealth. *Studies in health technology and informatics*, 121: 279.
- d'Aliberti, M. A., Olivia G. Clark. 2022. Preserving Patient Privacy During Computation over Shared Electronic Health Record Data. *Journal of Medical Systems*, 46(12): 85.
- Effah, C. Y.; Miao, R.; Drokow, E. K.; Agboyibor, C.; Qiao, R.; Wu, Y.; Miao, L.; and Wang, Y. 2022. Machine learning-assisted prediction of pneumonia based on non-invasive measures. *Frontiers in Public Health*, 10: 938801.
- Food, U. S.; and of Drugs, D. A. B. 1969. *National Drug Code Directory*. Consumer Protection and Environmental Health Service, Public Health Service . . .
- Gliklich, R.; Leavy, M.; and Dreyer, N. 2019. Tools and Technologies for Registry Interoperability, Registries for Evaluating Patient Outcomes: A User's Guide, Addendum 2.(Prepared by L&M Policy Research, LLC under Contract No. 290-2014-00004-C.) AHRQ Publication No. 19 (20)-EHC017-EF. *Rockville, MD: Agency for Healthcare Research and Quality*.
- Goodfellow, I. J.; Mirza, M.; Xiao, D.; Courville, A.; and Bengio, Y. 2015. An Empirical Investigation of Catastrophic Forgetting in Gradient-Based Neural Networks. arXiv:1312.6211.
- Guo, L. L.; Fries, J.; Steinberg, E.; Fleming, S. L.; Morse, K.; Aftandilian, C.; Posada, J.; Shah, N.; and Sung, L. 2024. A multi-center study on the adaptability of a shared foundation model for electronic health records. *NPJ Digital Medicine*, 7(1): 171.
- Guo, L. L.; Steinberg, E.; Fleming, S. L.; Posada, J.; Lemmon, J.; Pfohl, S. R.; Shah, N.; Fries, J.; and Sung, L. 2023.

- EHR foundation models improve robustness in the presence of temporal distribution shift. *Scientific Reports*, 13(1): 3767.
- Guze, L. B.; and Haley, L. D. 1958. Fungus infections of the urinary tract. *The Yale Journal of Biology and Medicine*, 30(4): 292.
- Harutyunyan, H.; Khachatrian, H.; Kale, D. C.; Ver Steeg, G.; and Galstyan, A. 2019. Multitask learning and benchmarking with clinical time series data. *Scientific data*, 6(1): 96.
- He, P.; Liu, X.; Gao, J.; and Chen, W. 2020. Deberta: Decoding-enhanced bert with disentangled attention. *arXiv preprint arXiv:2006.03654*.
- Huang, D.; Cogill, S.; Hsia, R. Y.; Yang, S.; and Kim, D. 2023. Development and external validation of a pretrained deep learning model for the prediction of non-accidental trauma. *npj Digital Medicine*, 6(1): 131.
- Johnson, A. E.; Bulgarelli, L.; Shen, L.; Gayles, A.; Sham-mout, A.; Horng, S.; Pollard, T. J.; Hao, S.; Moody, B.; Gow, B.; et al. 2023. MIMIC-IV, a freely accessible electronic health record dataset. *Scientific data*, 10(1): 1.
- Kaplan, J.; McCandlish, S.; Henighan, T.; Brown, T. B.; Chess, B.; Child, R.; Gray, S.; Radford, A.; Wu, J.; and Amodei, D. 2020. Scaling laws for neural language models. *arXiv preprint arXiv:2001.08361*.
- Kim, J.; Kim, J. S.; Kim, S.-H.; Yoo, S.; Lee, J. K.; and Kim, K. 2024. Deep learning-based prediction of Clostridioides difficile infection caused by antibiotics using longitudinal electronic health records. *NPJ Digital Medicine*, 7(1): 224.
- Kim, J.; Kim, J. S.; Lee, J.-H.; Kim, M.-G.; Kim, T.; Cho, C.; Park, R. W.; and Kim, K. 2025. Pretrained patient trajectories for adverse drug event prediction using common data model-based electronic health records. *Communications Medicine*, 5(1): 232.
- Levey, A. S.; and James, M. T. 2017. Acute kidney injury. *Annals of internal medicine*, 167(9): ITC66–ITC80.
- Li, Y.; Rao, S.; Solares, J. R. A.; Hassaine, A.; Ramakrishnan, R.; Canoy, D.; Zhu, Y.; Rahimi, K.; and Salimi-Khorshidi, G. 2020. BEHRT: transformer for electronic health records. *Scientific reports*, 10(1): 7155.
- Li, Z.; and Hoiem, D. 2017. Learning without forgetting. *IEEE transactions on pattern analysis and machine intelligence*, 40(12): 2935–2947.
- Liang, J.; Li, Y.; Zhang, Z.; Shen, D.; Xu, J.; Zheng, X.; Wang, T.; Tang, B.; Lei, J.; and Zhang, J. 2021. Adoption of electronic health records (EHRs) in China during the past 10 years: consecutive survey data analysis and comparison of Sino-American challenges and experiences. *Journal of medical Internet research*, 23(2): e24813.
- Liu, G.; Hsu, T.-M. H.; McDermott, M.; Boag, W.; Weng, W.-H.; Szolovits, P.; and Ghassemi, M. 2019. Clinically accurate chest x-ray report generation. In *Machine Learning for Healthcare Conference*, 249–269. PMLR.
- Liu, S.; Ma, W.; Moore, R.; Ganesan, V.; and Nelson, S. 2005. RxNorm: prescription for electronic drug information exchange. *IT professional*, 7(5): 17–23.
- Loshchilov, I.; and Hutter, F. 2017. Decoupled weight decay regularization. *arXiv preprint arXiv:1711.05101*.
- Mandair, D.; Tiwari, P.; Simon, S.; Colborn, K. L.; and Rosenberg, M. A. 2020. Prediction of incident myocardial infarction using machine learning applied to harmonized electronic health record data. *BMC medical informatics and decision making*, 20(1): 252.
- McCloskey, M.; and Cohen, N. J. 1989. Catastrophic Interference in Connectionist Networks: The Sequential Learning Problem. 24: 109–165.
- McDonald, C. J.; Huff, S. M.; Suico, J. G.; Hill, G.; Leavelle, D.; Aller, R.; Forrey, A.; Mercer, K.; DeMoor, G.; Hook, J.; et al. 2003. LOINC, a universal standard for identifying laboratory observations: a 5-year update. *Clinical chemistry*, 49(4): 624–633.
- Møller, J. K.; Sørensen, M.; and Hardahl, C. 2021. Prediction of risk of acquiring urinary tract infection during hospital stay based on machine-learning: A retrospective cohort study. *PloS one*, 16(3): e0248636.
- Nemati, S.; Holder, A.; Razmi, F.; Stanley, M. D.; Clifford, G. D.; and Buchman, T. G. 2018. An interpretable machine learning model for accurate prediction of sepsis in the ICU. *Critical care medicine*, 46(4): 547–553.
- Nusgart, M. 2018. Tips for Navigating the Healthcare Common Procedure Coding System Coding Process for New Devices.
- Parasrampur, S.; and Henry, J. 2019. Hospitals’ use of electronic health records data, 2015–2017. *ONC Data Brief*, 46(1): 13.
- Patterson, J. E.; and Andriole, V. T. 1997. Bacterial urinary tract infections in diabetes. *Infectious Disease Clinics*, 11(3): 735–750.
- Quan, H.; Sundararajan, V.; Halfon, P.; Fong, A.; Burnand, B.; Luthi, J.-C.; Saunders, L. D.; Beck, C. A.; Feasby, T. E.; and Ghali, W. A. 2005. Coding algorithms for defining comorbidities in ICD-9-CM and ICD-10 administrative data. *Medical care*, 43(11): 1130–1139.
- Rasmy, L.; Xiang, Y.; Xie, Z.; Tao, C.; and Zhi, D. 2021. Med-BERT: pretrained contextualized embeddings on large-scale structured electronic health records for disease prediction. *NPJ digital medicine*, 4(1): 86.
- Reinecke, I.; Zoch, M.; Reich, C.; Sedlmayr, M.; and Bathelt, F. 2021. The usage of OHDSI OMOP—a scoping review. *German Medical Data Sciences 2021: Digital Medicine: Recognize–Understand–Heal*, 95–103.
- Renc, P.; Jia, Y.; Samir, A. E.; Was, J.; Li, Q.; Bates, D. W.; and Sitek, A. 2024. Zero shot health trajectory prediction using transformer. *NPJ Digital Medicine*, 7(1): 256.
- Scherstén, B.; and Fritz, H. 1967. Subnormal levels of glucose in urine: a sign of urinary tract infection. *Jama*, 201(12): 949–952.
- Schick, T.; and Schütze, H. 2020. Exploiting cloze questions for few shot text classification and natural language inference. *arXiv preprint arXiv:2001.07676*.
- Sellergren, A.; Kazemzadeh, S.; Jaroensri, T.; Kiraly, A.; Traverse, M.; Kohlberger, T.; Xu, S.; Jamil, F.; Hughes, C.;

Lau, C.; Chen, J.; Mahvar, F.; Yatziv, L.; Chen, T.; Sterling, B.; Baby, S. A.; Baby, S. M.; Lai, J.; Schmidgall, S.; Yang, L.; Chen, K.; Björnsson, P.; Reddy, S.; Brush, R.; Philbrick, K.; Asiedu, M.; Mezerreg, I.; Hu, H.; Yang, H.; Tiwari, R.; Jansen, S.; Singh, P.; Liu, Y.; Azizi, S.; Kamath, A.; Ferret, J.; Pathak, S.; Vieillard, N.; Merhej, R.; Perrin, S.; Matejovicova, T.; Ramé, A.; Riviere, M.; Rouillard, L.; Mesnard, T.; Cideron, G.; bastien Grill, J.; Ramos, S.; Yvinec, E.; Casbon, M.; Buchatskaya, E.; Alayrac, J.-B.; Lepikhin, D.; Feinberg, V.; Borgeaud, S.; Andreev, A.; Hardin, C.; Dadashi, R.; Hussenot, L.; Joulin, A.; Bachem, O.; Matias, Y.; Chou, K.; Hassidim, A.; Goel, K.; Farabet, C.; Barral, J.; Warkentin, T.; Shlens, J.; Fleet, D.; Cotruta, V.; Sanseviero, O.; Martins, G.; Kirk, P.; Rao, A.; Shetty, S.; Steiner, D. F.; Kirmizibayrak, C.; Pilgrim, R.; Golden, D.; and Yang, L. 2025. MedGemma Technical Report. *arXiv:2507.05201*.

Stang, P. E.; Ryan, P. B.; Racoosin, J. A.; Overhage, J. M.; Hartzema, A. G.; Reich, C.; Welebob, E.; Scarnecchia, T.; and Woodcock, J. 2010. Advancing the science for active surveillance: rationale and design for the Observational Medical Outcomes Partnership. *Annals of internal medicine*, 153(9): 600–606.

Su, X.; Messica, S.; Huang, Y.; Johnson, R.; Fesser, L.; Gao, S.; Sahneh, F.; and Zitnik, M. 2025. Multimodal Medical Code Tokenizer. *arXiv preprint arXiv:2502.04397*.

Wan, Z.; Liu, C.; Wang, X.; Tao, C.; Shen, H.; Peng, Z.; Fu, J.; Arcucci, R.; Yao, H.; and Zhang, M. 2024. MEIT: Multi-modal electrocardiogram instruction tuning on large language models for report generation. *arXiv preprint arXiv:2403.04945*.

Wornow, M.; Thapa, R.; Steinberg, E.; Fries, J.; and Shah, N. 2023. Ehrshot: An ehr benchmark for few-shot evaluation of foundation models. *Advances in Neural Information Processing Systems*, 36: 67125–67137.

Yang, Z.; Mitra, A.; Liu, W.; Berlowitz, D.; and Yu, H. 2023. TransformEHR: transformer-based encoder-decoder generative model to enhance prediction of disease outcomes using electronic health records. *Nature communications*, 14(1): 7857.

Zhang, H.; Yang, X.; Bai, L.; and Liang, J. 2023a. Enhancing drug recommendations via heterogeneous graph representation learning in EHR networks. *IEEE Transactions on Knowledge and Data Engineering*, 36(7): 3024–3035.

Zhang, Y.; Zhu, H.; Song, Z.; Koniusz, P.; King, I.; et al. 2023b. Mitigating the popularity bias of graph collaborative filtering: A dimensional collapse perspective. *Advances in Neural Information Processing Systems*, 36: 67533–67550.

Zhu, Y.; Xu, Y.; Yu, F.; Liu, Q.; Wu, S.; and Wang, L. 2020. Deep graph contrastive representation learning. *arXiv preprint arXiv:2006.04131*.

Author contributions

Junmo Kim and Namkyeong Lee contributed to the conceptualization and design of the study. Junmo Kim handled and mainly analyzed the research data, and all authors interpreted the results. Junmo Kim organized deep learning models and LLM implementation. Junmo Kim wrote the original draft of the paper. Junmo Kim and Jiwon Kim made figures. Kwangsoo Kim supervised the study and provided computational resources. All authors had the final responsibility to submit for publication.

Author contributions

This research was supported and funded by SNUH Lee Kun-hee Child Cancer & Rare Disease Project, Republic of Korea (grant number : 22A-000-0000).

Competing interests

All authors declare no competing interests.

Data Availability

All data used in this study is publicly available. The data generated and analyzed during the study are available from the corresponding author upon reasonable request.

Code Availability

The codes for the study were based on our GitHub repository (<https://github.com/kicarussays/MedRep>).

Supplementary Materials

Supplementary Table 1. Downstream task performance. All downstream tasks were performed with three random seeds and all values are shown as mean \pm SD.

Representation	MT	LLOS	RA	Pheno	UTI	Fx	Sepsis	PNA	MI
<i>Metric: AUROC</i>									
<i>Internal Validation</i>									
None	0.857 ± 0.030	0.767 ± 0.018	0.751 ± 0.041	0.741 ± 0.004	0.836 ± 0.010	0.772 ± 0.019	0.791 ± 0.005	0.817 ± 0.006	0.789 ± 0.011
MedTok	0.894 ± 0.007	0.817 ± 0.014	0.700 ± 0.048	0.764 ± 0.005	0.857 ± 0.007	0.811 ± 0.021	0.828 ± 0.017	0.855 ± 0.006	0.844 ± 0.003
MedRep	0.926 ± 0.014	0.845 ± 0.004	0.747 ± 0.045	0.766 ± 0.002	0.873 ± 0.004	0.857 ± 0.007	0.853 ± 0.005	0.871 ± 0.005	0.855 ± 0.008
<i>External Validation</i>									
None	0.730 ± 0.015	0.636 ± 0.016	0.607 ± 0.006	0.643 ± 0.012	0.795 ± 0.022	0.688 ± 0.013	0.777 ± 0.024	0.808 ± 0.016	0.705 ± 0.019
MedTok	0.803 ± 0.021	0.677 ± 0.007	0.580 ± 0.038	0.632 ± 0.009	0.811 ± 0.002	0.824 ± 0.013	0.827 ± 0.013	0.862 ± 0.005	0.783 ± 0.005
MedRep	0.883 ± 0.009	0.753 ± 0.016	0.652 ± 0.022	0.664 ± 0.011	0.823 ± 0.006	0.879 ± 0.015	0.844 ± 0.005	0.865 ± 0.003	0.816 ± 0.036
<i>Metric: AUPRC</i>									
<i>Internal Validation</i>									
None	0.272 ± 0.062	0.558 ± 0.034	0.149 ± 0.113	0.297 ± 0.009	0.577 ± 0.041	0.184 ± 0.018	0.283 ± 0.023	0.403 ± 0.028	0.111 ± 0.021
MedTok	0.353 ± 0.011	0.647 ± 0.017	0.101 ± 0.045	0.317 ± 0.001	0.605 ± 0.039	0.377 ± 0.006	0.421 ± 0.045	0.524 ± 0.011	0.224 ± 0.031
MedRep	0.443 ± 0.027	0.693 ± 0.028	0.191 ± 0.107	0.308 ± 0.007	0.642 ± 0.033	0.466 ± 0.023	0.510 ± 0.021	0.590 ± 0.023	0.273 ± 0.046
<i>External Validation</i>									
None	0.165 ± 0.016	0.395 ± 0.007	0.132 ± 0.000	0.243 ± 0.011	0.599 ± 0.045	0.155 ± 0.005	0.459 ± 0.077	0.501 ± 0.038	0.227 ± 0.050
MedTok	0.233 ± 0.027	0.438 ± 0.012	0.119 ± 0.012	0.237 ± 0.005	0.661 ± 0.001	0.612 ± 0.042	0.598 ± 0.051	0.747 ± 0.014	0.377 ± 0.054
MedRep	0.445 ± 0.004	0.539 ± 0.026	0.158 ± 0.014	0.246 ± 0.004	0.664 ± 0.003	0.738 ± 0.026	0.710 ± 0.035	0.772 ± 0.005	0.472 ± 0.145

Supplementary Table 2. Downstream task performance on Med-BERT. All downstream tasks were performed with three random seeds and all values are shown as mean \pm SD.

Representation	MT	LLOS	RA	Pheno	UTI	Fx	Sepsis	PNA	MI
<i>Metric: AUROC</i>									
<i>Internal Validation</i>									
None	0.828 ± 0.040	0.767 ± 0.016	0.662 ± 0.094	0.742 ± 0.002	0.820 ± 0.010	0.752 ± 0.005	0.783 ± 0.001	0.808 ± 0.015	0.773 ± 0.037
MedTok	0.878 ± 0.008	0.807 ± 0.011	0.722 ± 0.070	0.753 ± 0.006	0.849 ± 0.009	0.818 ± 0.013	0.814 ± 0.005	0.835 ± 0.012	0.842 ± 0.023
MedRep	0.899 ± 0.007	0.806 ± 0.020	0.769 ± 0.045	0.762 ± 0.003	0.859 ± 0.005	0.842 ± 0.017	0.840 ± 0.015	0.852 ± 0.001	0.855 ± 0.014
<i>External Validation</i>									
None	0.637 ± 0.072	0.629 ± 0.005	0.569 ± 0.013	0.618 ± 0.005	0.814 ± 0.006	0.644 ± 0.018	0.785 ± 0.038	0.825 ± 0.011	0.678 ± 0.040
MedTok	0.806 ± 0.007	0.665 ± 0.029	0.634 ± 0.008	0.653 ± 0.023	0.811 ± 0.004	0.845 ± 0.031	0.773 ± 0.010	0.795 ± 0.016	0.783 ± 0.014
MedRep	0.826 ± 0.016	0.713 ± 0.026	0.621 ± 0.004	0.647 ± 0.023	0.814 ± 0.002	0.861 ± 0.010	0.825 ± 0.018	0.866 ± 0.006	0.790 ± 0.027
<i>Metric: AUPRC</i>									
<i>Internal Validation</i>									
None	0.223 ± 0.034	0.562 ± 0.021	0.097 ± 0.062	0.293 ± 0.005	0.563 ± 0.038	0.173 ± 0.013	0.329 ± 0.051	0.426 ± 0.023	0.143 ± 0.043
MedTok	0.310 ± 0.010	0.631 ± 0.019	0.152 ± 0.133	0.304 ± 0.005	0.592 ± 0.031	0.322 ± 0.014	0.352 ± 0.019	0.422 ± 0.013	0.195 ± 0.037
MedRep	0.381 ± 0.040	0.642 ± 0.036	0.132 ± 0.068	0.310 ± 0.010	0.612 ± 0.035	0.401 ± 0.012	0.471 ± 0.044	0.544 ± 0.011	0.215 ± 0.002
<i>External Validation</i>									
None	0.148 ± 0.020	0.371 ± 0.007	0.115 ± 0.005	0.224 ± 0.008	0.648 ± 0.005	0.148 ± 0.006	0.484 ± 0.132	0.629 ± 0.034	0.272 ± 0.110
MedTok	0.238 ± 0.012	0.427 ± 0.020	0.134 ± 0.009	0.245 ± 0.021	0.654 ± 0.006	0.624 ± 0.073	0.472 ± 0.035	0.516 ± 0.036	0.359 ± 0.063
MedRep	0.342 ± 0.032	0.478 ± 0.025	0.137 ± 0.001	0.243 ± 0.015	0.654 ± 0.009	0.655 ± 0.033	0.658 ± 0.055	0.762 ± 0.004	0.356 ± 0.084

Supplementary Table 3. Downstream task performance on CDM-BERT. All downstream tasks were performed with three random seeds and all values are shown as mean \pm SD

Representation	MT	LLOS	RA	Pheno	UTI	Fx	Sepsis	PNA	MI
<i>Metric: AUROC</i>									
<i>Internal Validation</i>									
None	0.862 ± 0.010	0.811 ± 0.020	0.730 ± 0.062	0.746 ± 0.003	0.852 ± 0.005	0.750 ± 0.026	0.791 ± 0.042	0.836 ± 0.011	0.730 ± 0.059
MedTok	0.879 ± 0.012	0.824 ± 0.013	0.740 ± 0.143	0.741 ± 0.003	0.855 ± 0.010	0.818 ± 0.015	0.835 ± 0.010	0.849 ± 0.008	0.843 ± 0.011
MedRep	0.928 ± 0.011	0.858 ± 0.006	0.733 ± 0.033	0.766 ± 0.007	0.869 ± 0.005	0.837 ± 0.017	0.848 ± 0.003	0.871 ± 0.007	0.862 ± 0.019
<i>External Validation</i>									
None	0.770 ± 0.004	0.699 ± 0.010	0.597 ± 0.025	0.623 ± 0.021	0.810 ± 0.002	0.714 ± 0.037	0.844 ± 0.007	0.840 ± 0.017	0.703 ± 0.054
MedTok	0.842 ± 0.015	0.700 ± 0.014	0.631 ± 0.027	0.639 ± 0.025	0.800 ± 0.006	0.842 ± 0.012	0.849 ± 0.005	0.855 ± 0.003	0.802 ± 0.011
MedRep	0.876 ± 0.013	0.764 ± 0.008	0.626 ± 0.023	0.645 ± 0.009	0.819 ± 0.005	0.873 ± 0.003	0.859 ± 0.007	0.865 ± 0.014	0.826 ± 0.007
<i>Metric: AUPRC</i>									
<i>Internal Validation</i>									
None	0.318 ± 0.076	0.621 ± 0.037	0.130 ± 0.047	0.291 ± 0.004	0.606 ± 0.041	0.235 ± 0.011	0.415 ± 0.006	0.471 ± 0.038	0.194 ± 0.060
MedTok	0.394 ± 0.015	0.669 ± 0.018	0.136 ± 0.110	0.290 ± 0.000	0.623 ± 0.042	0.427 ± 0.030	0.504 ± 0.009	0.546 ± 0.007	0.256 ± 0.019
MedRep	0.438 ± 0.021	0.715 ± 0.019	0.096 ± 0.042	0.312 ± 0.004	0.626 ± 0.032	0.413 ± 0.011	0.514 ± 0.025	0.598 ± 0.014	0.328 ± 0.044
<i>External Validation</i>									
None	0.226 ± 0.018	0.482 ± 0.009	0.118 ± 0.010	0.225 ± 0.019	0.649 ± 0.004	0.239 ± 0.005	0.720 ± 0.012	0.664 ± 0.061	0.364 ± 0.029
MedTok	0.324 ± 0.020	0.482 ± 0.015	0.126 ± 0.014	0.234 ± 0.020	0.643 ± 0.003	0.694 ± 0.019	0.749 ± 0.003	0.768 ± 0.005	0.508 ± 0.017
MedRep	0.400 ± 0.040	0.563 ± 0.012	0.136 ± 0.018	0.243 ± 0.009	0.663 ± 0.001	0.720 ± 0.003	0.750 ± 0.016	0.772 ± 0.015	0.552 ± 0.008

Supplementary Table 4. Medical vocabularies included in MedRep.

Vocabulary	Count	Vocabulary	Count
RxNorm Extension	2145325	CIM10	14223
NDC	1183702	ICD9ProcCN	13385
SPL	720063	CCAM	10206
SNOMED	531174	OPCS4	9821
RxNorm	308709	Multum	9770
EDI	293618	CTD	8698
OMOP Genomic	289889	ClinVar	8072
Nebraska Lexicon	268995	JAX	7855
ICD10PCS	196221	OXMIS	7083
dm+d	192706	ATC	6740
DPD	188287	Cancer Modifier	6028
LOINC	155903	HemOnc	5786
AMT	130006	OncoKB	5569
ICD10CM	88467	CGI	5351
Read	74816	ICD9Proc	4657
NDFRT	69566	SNOMED Veterinary	4009
KDC	63749	SUS	3914
ICDO3	62535	HCPCS	3422
NCCD	51547	UK Biobank	2725
CIEL	48544	NCIt	2426
BDPM	43214	NAACCR	2173
OPS	42959	CIViC	1386
JMDC	37485	OMOP Extension	1189
ICD10CN	31309	EphMRA ATC	895
OMOP Invest Drug	29727	OncoTree	885
GCN_SEQNO	29659	NFC	692
VANDF	29351	VA Class	576
GGR	25849	CO-CONNECT TWINS	449
MeSH	24376	SMQ	324
KCD7	20010	CVX	271
ICD10GM	16250	CO-CONNECT	137
ICD9CM	15585	PPI	109
ICD10	14411	Cohort	78

Supplementary Table 5. Prompt for each domain of OMOP vocabulary and example descriptions.

Domain	Prompt (with example concept)	Description
Condition	Instruction: Briefly explain the clinical background and regarding treatments of each concept name (condition) with less than 5 sentences. Do not include sentences that are too ordinary (such as "further details would depend on the specific situation) and focus on describing the representative clinical features of the concept. Concept name: Neutropenic fever	Neutropenic fever occurs in patients with neutropenia, characterized by an abnormally low level of neutrophils, often due to chemotherapy, bone marrow disorders, or immunosuppression. Clinically, it presents as a fever, which can be the only sign of infection in these patients due to their compromised immune response. The absence of typical signs of infection, such as pus formation or localized symptoms, can make diagnosis challenging. Treatment involves prompt administration of broad-spectrum antibiotics to mitigate the risk of severe infections, and in some cases, granulocyte-colony stimulating factors (G-CSF) may be used to expedite neutrophil recovery. Monitoring for potential complications, such as sepsis, is crucial in the management of neutropenic fever.
Drug	Instruction: Briefly explain the clinical background and purpose of each concept name (drug) with less than 5 sentences. Do not include sentences that are too ordinary (such as "further details would depend on the specific situation) and focus on describing the representative clinical features of the concept. For explanation, if it exists in the concept name, take into account the detailed items of the concept such as ingredient, dosage form, and strength. If several drugs are contained in a concept, do not explain those drugs separately, but explain the concept name comprehensively and finish the answer with less than 5 sentences. Concept name: Aspirin 100 MG Oral Tablet [Aspirin]	Aspirin 100 MG Oral Tablet is a low-dose formulation of acetylsalicylic acid, primarily used for its antiplatelet effects to reduce the risk of cardiovascular events such as heart attacks and strokes. This dosage is particularly effective in the long-term management of patients with a history of cardiovascular disease or those at high risk. Additionally, aspirin has anti-inflammatory and analgesic properties, making it useful in managing certain inflammatory conditions and mild to moderate pain. The 100 MG strength is often chosen to minimize gastrointestinal side effects while providing adequate antithrombotic benefits. Regular use under a healthcare provider's guidance is crucial for balancing benefits and potential risks.
Measurement	Instruction: Briefly explain the clinical background and context of each concept name (measurement) with less than 5 sentences. Do not include sentences that are too ordinary (such as "further details would depend on the specific situation) and focus on describing the representative clinical features of the concept. For explanation, if it exists in the concept name, describe what the decile means clinically. Concept name: Glycated haemoglobin (HbA1c) (9th decile)	Glycated hemoglobin (HbA1c) is a measure of average blood glucose levels over the past two to three months, reflecting long-term glycemic control in individuals with diabetes. A value in the 9th decile typically indicates a HbA1c level of approximately 8.0% to 9.0%, suggesting poorly controlled diabetes and an increased risk for microvascular and macrovascular complications, such as retinopathy and cardiovascular disease. Clinically, this decile serves as a critical threshold for considering more aggressive therapeutic interventions, including medication adjustments and comprehensive diabetes management strategies. Monitoring HbA1c in this range underscores the importance of lifestyle modifications and personalized treatment plans to improve glycemic control and reduce long-term health risks.
Procedure	Instruction: Briefly explain the clinical background and purpose of each concept name (procedure) with less than 5 sentences. Do not include sentences that are too ordinary (such as "further details would depend on the specific situation) and focus on describing the representative clinical features of the concept. Concept name: Holter extended electrocardiographic recording	Holter extended electrocardiographic recording is a continuous monitoring technique that captures the heart's electrical activity over 24 to 48 hours using a portable ECG device. This procedure is essential for diagnosing arrhythmias, assessing symptoms like palpitations, and evaluating the efficacy of antiarrhythmic medications. Patients wear the device during their daily activities, allowing for a comprehensive assessment of heart rhythm in real-life settings rather than just during a brief clinical visit. Analysis of the recorded data can reveal transient abnormalities or patterns that might not be evident during a standard ECG.

Supplementary Table 6. Configuration for GRACE

Configuration	Value
Batch size	1024
Learning rate	0.0005
Hidden size	768
Activation function	pReLU
Graph neural network	Graph convolutional networks
Number of layers	2
Dropout rate	0.2
DropEdge rate	0.2
τ	0.5
Max epoch	200
Early stopping patience	20